

# Spin exchange and superconductivity in a $t - J' - V$ model for two-dimensional quarter-filled systems

Andrés Greco<sup>1</sup>, Jaime Merino<sup>2</sup>, Adriana Foussats<sup>3</sup> and Ross H. McKenzie<sup>4</sup>

<sup>1,3</sup> *Facultad de Ciencias Exactas, Ingeniería y Agrimensura and Instituto de Física Rosario (UNR-CONICET). Av. Pellegrini 250-2000. Rosario-Argentina.*

<sup>2</sup> *Departamento de Física Teórica de la Materia Condensada, Universidad Autónoma de Madrid, Madrid 28049, Spain.*

<sup>4</sup> *Department of Physics, University of Queensland, Brisbane 4072, Australia.*  
(Dated: March 22, 2018)

The effect of antiferromagnetic spin fluctuations on two-dimensional quarter-filled systems is studied theoretically. An effective  $t - J' - V$  model on a square lattice which accounts for checkerboard charge fluctuations and next-nearest-neighbors antiferromagnetic spin fluctuations is considered. From calculations based on large- $N$  theory on this model it is found that the exchange interaction,  $J'$ , increases the attraction between electrons in the  $d_{xy}$  channel only, so that both charge and spin fluctuations work cooperatively to produce  $d_{xy}$  pairing.

PACS numbers: 71.27.+a, 71.10.Fd, 74.70.Kn, 71.45.Lr

## I. INTRODUCTION

The BEDT-TTF (bis-ethylenedithiotetrathiafulvalene) family of quarter-filled layered organic materials with the  $\theta$ ,  $\alpha$  and  $\beta''$  arrangements of the molecules display a subtle competition between metallic, charge ordered insulating and superconducting phases<sup>1,2</sup>. They are examples of strongly correlated electron systems for which their electronic states are theoretically described by a 2D extended Hubbard model at 3/4-filling of electrons (1/4-filling of holes) for the HOMO of the BEDT-TTF molecules<sup>3</sup>. The nearest-neighbors intermolecular Coulomb interaction,  $V$ , is a crucial ingredient as, at one-quarter filling, the on site Coulomb repulsion,  $U$ , by itself cannot describe charge ordering phenomena<sup>4</sup>. The extended Hubbard model at this filling has been previously studied<sup>2</sup> through large- $N$  and slave-boson approaches in the  $U$ -infinite limit as well as with exact diagonalization on small clusters<sup>5</sup> at finite- $U$ . Several issues related to charge ordering phenomena have been addressed. A transition from a metal to a checkerboard charge ordered insulating state at a finite  $V = V_c$  has been found. Close to this charge ordered phase, superconductivity in the  $d_{xy}$  channel appears<sup>6</sup> induced by strong charge fluctuations. Dynamical<sup>7</sup> properties of the metallic phase in the presence of short range charge fluctuations have been found to be anomalous in agreement with experimental data<sup>8</sup>.

Large- $N$  methods and slave bosons are useful for the study of the effect of charge fluctuations on various electronic properties as they can be included at  $O(1/N)$ , however, spin fluctuations are typically neglected unless complicated  $O(1/N^2)$  contributions are considered. The effect of spin fluctuations on superconductivity in quarter-filled systems has been addressed through RPA (Random Phase Approximation) calculations which consider antiferromagnetic instabilities induced by the on-site Coulomb interaction,  $U$  [9], finding that  $d_{xy}$  superconductivity still prevails. However, well in the charge ordered insulating phase it is known that the spins or-

der antiferromagnetically due to the presence of a next-nearest neighbor spin exchange interaction<sup>2</sup>. This spin interaction results from a 'ring' exchange process appearing at fourth order in  $t$  and acts along the diagonals of the square lattice reading:  $J' = 4t^4/9V^3$  in the  $U \rightarrow \infty$ , and  $V \gg t$  limits. Exact diagonalization on 16-site clusters indicate that the  $(\pi/2, \pi/2)$  antiferromagnetic spin arrangement follows closely the  $(\pi, \pi)$  checkerboard arrangement of the charge<sup>10</sup> as  $V/t$  is increased from the metal to the charge ordered phase. These results suggest that remnants of the exchange interaction,  $J'$ , generated in the insulating phase can survive in the metallic phase where short range charge ordering is present. It is then the purpose of the present work to analyze the influence of this exchange coupling,  $J'$ , on the superconducting instabilities previously found<sup>6</sup> induced by charge fluctuations. As this  $J'$  acts along the diagonals of the lattice it is conceivable that similarly to the  $d_{x^2-y^2}$  superconductivity appearing in the  $t - J$  model close to half-filling induced by antiferromagnetic spin fluctuations, the  $J'$  appearing in the quarter-filled  $t - J' - V$  model can induce  $d_{xy}$  pairing.

The paper is organized as follows. In Sect. II we introduce the quarter-filled  $t - J' - V$  model and provide a phase diagram obtained from the large- $N$  approach used here. In Sect. III we discuss the superconducting phase and study in detail the effect of  $J'$  on the pairing symmetry. Finally in Sect. IV we summarize our results and point out their connection to the electronic properties of quarter-filled layered organic molecular crystals.

## II. THE $t - J' - V$ MODEL AND ITS PHASE DIAGRAM

In order to explore the above possibility an effective quarter-filled  $t - J' - V$  model is introduced as a natural extension of the extended Hubbard model previously studied (see Fig. 1 for a schematic sketch of the effective

interactions). The model reads

$$H = \sum_{\langle ij \rangle, \sigma} (t_{ij} \tilde{c}_{i\sigma}^\dagger \tilde{c}_{j\sigma} + h.c.) + \sum_{\langle ij \rangle} J'_{ij} (\vec{S}_i \cdot \vec{S}_j - \frac{1}{4} n_i n_j) + \sum_{\langle ij \rangle} V_{ij} n_i n_j, \quad (1)$$

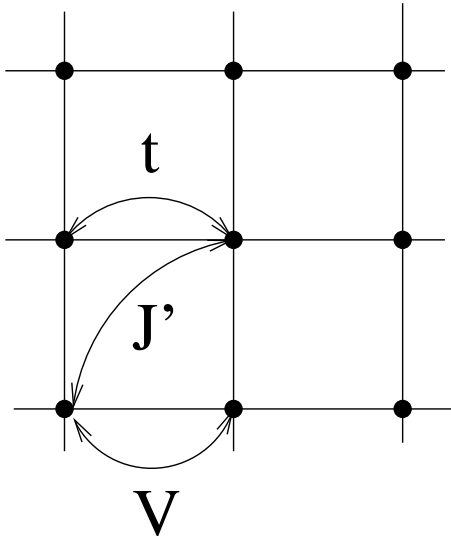


FIG. 1: A square lattice with a nearest-neighbors Coulomb repulsion  $V$  and hopping amplitude  $t$  and a next-nearest neighbors spin exchange coupling  $J'$ .

where  $t_{ij}$  and  $V_{ij}$  are the nearest-neighbors hopping and Coulomb repulsion parameters, respectively, between sites  $i$  and  $j$  on the square lattice.  $J'_{ij}$  is the antiferromagnetic exchange interaction between second-neighbors sites.  $\tilde{c}_{i\sigma}^\dagger$  and  $\tilde{c}_{i\sigma}$  are the fermionic creation and destruction operators respectively under the constraint that double occupancies of lattice sites  $i$  are excluded.  $\vec{S}_i$  and  $n_i$  are the spin and the fermionic density, respectively.

The model (1) is studied by using the large- $N$  approach for Hubbard operators<sup>11</sup> recently extended to the case of finite  $J$ <sup>12</sup> (see also Ref.[7] for the  $J = 0$  case). In the appendix we give details about this approach. The method has been thoroughly tested on the  $t - U - V$  model by comparing dynamical properties with exact diagonalization calculations on small clusters<sup>7</sup>, finding good agreement for the behavior of charge and spectral functions as well as spectral densities close to the charge ordering transition. This agreement can be attributed to the fact that the infinite- $U$  limit has been considered and neglecting the nearest-neighbor exchange  $J$  is justified since, at finite  $V$ , the charge tries to sit in every other site of the square lattice making  $J$  ineffective.

Although the  $t - J' - V$ -model is only justified for values of  $V$  sufficiently large, we have explored the full param-

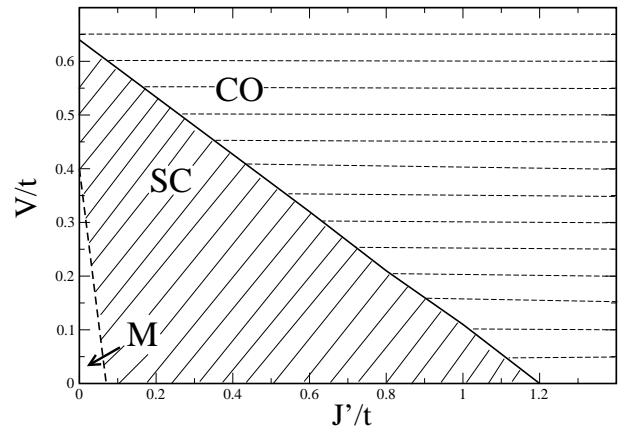


FIG. 2: Phase diagram obtained from the large- $N$  approach in the  $V - J'$  plane. The solid line represents  $V_c$  *i. e.* the critical line signalling the onset of checkerboard charge ordering (CO). Between the solid and dashed lines  $d_{xy}$  superconductivity (SC) appears. The region below the dashed line corresponds to the metallic (M) phase. Superconductivity is found to be more robust closer to the CO line and for larger  $J'$ .

eter range for completeness. In the  $t - J' - V$  model, the  $J'$  is dynamically generated when the charge is ordered within the checkerboard pattern through a 'ring' exchange process. Hence, the  $J'$  becomes effective only when some sort of checkerboard charge ordering is already present in the system (either short or long range charge order). This means that the system should be charge ordered or sufficiently close to the charge ordering transition for the  $t - J' - V$  model to be meaningful. The situation is different in the  $t - J$  model for the high- $T_c$  as, in this case, the  $J$  is generated through a super-exchange process at large on-site  $U$ .

A full phase diagram summarizing our results obtained from large- $N$  theory on the  $t - J' - V$  model is shown in Fig. 2, where metallic (M), charge ordered (CO) and superconducting (SC) phases occur. We start with a discussion of the charge ordering transition. The critical value,  $V_c$ , signalling the charge ordering (CO) transition of the metallic phase as obtained from the divergence of the static charge susceptibility (see appendix), is displayed as a solid line in Fig. 2. For  $J' = 0$ , the system charge orders at  $V = V_c \sim 0.65t$ , as previously found<sup>2,7</sup>. The value of  $V_c$  is found to decrease with increasing  $J'$  which can be easily understood from the following. By increas-

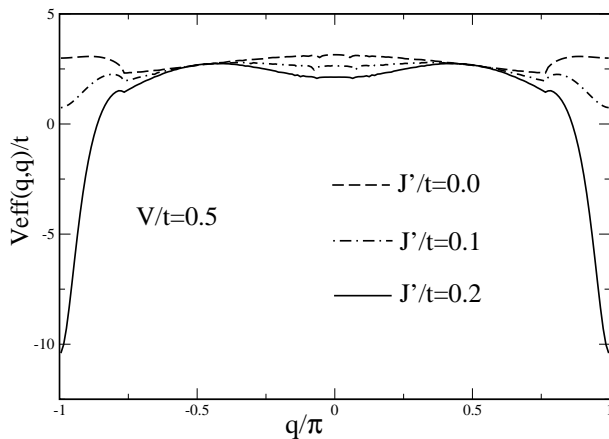


FIG. 3: Behavior of the effective potential between quasiparticles,  $V_{eff}(q, q)$ , for  $J' = 0$ ,  $J' = 0.1t$  and  $J' = 0.2t$ , for fixed  $V = 0.5t$ . For this parameters the system is within the metallic phase close to the charge ordering transition (see phase diagram in Fig. 2). As  $J'$  is increased,  $V_{eff}(q, q)$  becomes more anisotropic and more attractive near the momentum transfer  $\mathbf{q} \sim (\pi, \pi)$ . Divergences appearing at  $(\pi, \pi)$  for increasing  $J'$  favor superconductivity in the  $d_{xy}$  channel.

ing  $J'$ , checkerboard charge ordering is favored because two electrons are antiferromagnetically attracted when they are sitting along the diagonals of the square lattice so that a smaller  $V$  is effectively needed to induce CO. In a similar way, if we switch on  $J'$  for a fixed  $V \lesssim V_c$ , the CO phase is favored. The dashed-dotted line in Fig. 2 marks the onset for superconductivity. Between solid and dashed lines the superconducting effective coupling in the  $d_{xy}$  channel (see below) becomes negative indicative of superconducting pairing. Superconductivity in the  $d_{xy}$  channel is found to be more robust for larger  $J'$  and closer to CO, as one would expect as in either way a stronger attraction is felt between quasiparticles in every other site of the lattice.

### III. SUPERCONDUCTIVITY IN THE $t - J' - V$ MODEL

In order to understand the model proposed we first discuss related large- $N$  studies performed in the well known models such as the  $t - J$  model relevant to the cuprates. The case of a nearest-neighbors exchange coupling,  $J$ , has been studied using a Slave-boson techniques have been used in combination with a  $1/N$  expansion to study

superconducting instabilities on  $t - J$  model<sup>13</sup> and Hubbard model<sup>14</sup>. Both the present approach (as described in the appendix) and the slave-boson one, to  $O(1)$ , lead to fermions renormalized by the presence of the Coulomb interaction. Indeed, superconductivity in the model can only appear at  $O(1/N)$ . By adding an extra  $J'$  term to the bare extended Hubbard hamiltonian ( $t - J' - V$ -model) we can treat both  $J'$  and  $V$ -terms at the same level of approximation, *i. e.* through  $O(1/N)$  and analyze possible superconducting instabilities. A closely related work by Vojta<sup>15</sup> analyzes recently coexistence of superconductivity and checkerboard charge ordering within a  $t - J - V$  model close to half-filling relevant to STM experiments on the cuprates<sup>16</sup>.

Superconductivity is then investigated, within our model, by calculating the effective interaction,  $V_{eff}(\mathbf{q})$ , through  $O(1/N)$  (see appendix), between fermions for finite  $J'$  at one-quarter filling. The potential,  $V_{eff}(\mathbf{q})$  is plotted along the  $\mathbf{q} = (q, q)$  direction in Fig. 3 as a function of  $q$  for different  $J'$ :  $J' = 0$ ,  $J' = 0.1t$  and  $J' = 0.2t$ , and fixed  $V = 0.5t$ . For this set of parameters the system is always metallic but close to the charge ordering transition as can be seen from Fig. 2. For  $J' = 0$ ,  $V_{eff}(\mathbf{q})$  is repulsive and anisotropic as found previously (see Fig. 13 of Ref.[7]). As  $J'$  is increased,  $V_{eff}(q, q)$  becomes more anisotropic and more attractive near the momentum transfer  $\mathbf{q} \sim (\pi, \pi)$ . This behavior favors superconductivity in the  $d_{xy}$  channel as the  $J'$  attracts the charge tending to form the checkerboard pattern along the diagonals of the square lattice.

There are two kinds of interactions contributing to  $V_{eff}(\mathbf{q})$ . For  $J' = 0$ , the effective interaction close to CO is mainly dominated by charge fluctuations associated with the collective excitations near  $(\pi, \pi)$ <sup>7</sup>. Therefore, this kind of pairing interaction, like the phonon mechanism in simple metals, is mainly retarded and occurs in momentum space. For  $V = 0$ , the main effective interaction is of magnetic origin, unretarded and short range in real space. For  $J'$  and  $V$  different from zero both kind of interactions contribute cooperatively to the binding energy of the Cooper pairs.

We use this effective potential to compute the effective couplings in the different pairing channels or irreducible representations of the order parameter,  $i$  ( $i = (d_{x^2-y^2}, d_{xy}, p)$ ). In this way we can project out the interaction with a certain symmetry. The critical temperatures,  $T_c$ , can then be estimated in weak coupling from:  $T_{ci} = 1.13\omega_0 \exp(-1/|\lambda_i|)$ , where  $\omega_0$  is a suitable cutoff frequency and  $\lambda_i$  are the effective couplings with different symmetries. These are defined as<sup>7</sup>:

$$\lambda_i = \frac{1}{(2\pi)^2} \frac{\int (d\mathbf{k}/|v_{\mathbf{k}}|) \int (d\mathbf{k}'/|v_{\mathbf{k}'}|) g_i(\mathbf{k}') V_{eff}(\mathbf{k}' - \mathbf{k}) g_i(\mathbf{k})}{\int (d\mathbf{k}/|v_{\mathbf{k}}|) g_i(\mathbf{k})^2} \quad (2)$$

where the functions  $g_i(\mathbf{k})$ , encode the different pairing

symmetries, and  $v_{\mathbf{k}}$  are the quasiparticle velocities at

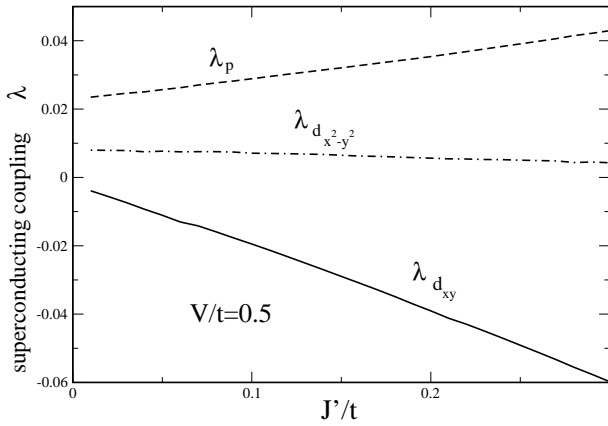


FIG. 4: The dimensionless superconducting coupling  $\lambda$  in the  $p$  ( $\lambda_p$ ) (dashed line),  $d_{x^2-y^2}$  ( $\lambda_{d_{x^2-y^2}}$ ) (dashed-dotted line) and  $d_{xy}$  ( $\lambda_{d_{xy}}$ ) (solid line) channels as a function of  $J'$  for a given value of  $V = 0.5t$  in the metallic phase close to the CO instability. The second-neighbors antiferromagnetic exchange,  $J'$ , favors superconductivity in the  $d_{xy}$  channel only.

the Fermi surface. The integrations are restricted to the Fermi surface.  $\lambda_i$  measures the strength of the interaction between electrons at the Fermi surface in a given symmetry channel  $i$ . If  $\lambda_i > 0$ , electrons are repelled. Hence, superconductivity is only possible when  $\lambda_i < 0$ .

The coupling strength  $\lambda$  for  $d_{xy}$  superconductivity has been found<sup>6,7</sup> to be very small (see Fig. 15 of Ref.[7]) previously. For these small couplings, the corresponding superconducting critical temperature  $T_c$  is predicted to be very low. Other indications for pairing come from exact diagonalization calculations of the binding energy of two holes which becomes negative near the charge ordering transition<sup>7</sup>. In Fig. 4 we present results for the dimensionless superconducting coupling  $\lambda$  in the  $p$  ( $\lambda_p$ ),  $d_{x^2-y^2}$  ( $\lambda_{d_{x^2-y^2}}$ ) and  $d_{xy}$  ( $\lambda_{d_{xy}}$ ) channels as a function of  $J'$  for a given value of  $V = 0.5t$  close to the CO instability.

Clearly, superconductivity becomes more favorable in the  $d_{xy}$  channel only as  $J'$  is increased. The influence of  $J'$  on the  $d_{x^2-y^2}$ -symmetry (dashed-dotted line in Fig. 4) is rather weak. When  $J'$  increases, superconducting couplings are more repulsive in the  $p$ -channel and even more in the  $s$ -symmetry (not shown) channel.

Note also the large difference between the  $\lambda$  values for  $J' = 0$ <sup>7</sup> and  $J' = 0.3t$ . For  $J' = 0.3t$ ,  $\lambda$  is one order of magnitude larger than for  $J' = 0$  at  $V = 0.5t$ . This behavior, which only occurs in the  $d_{xy}$  channel, shows the strong influence of the second neighbors effective antiferromagnetic exchange coupling  $J'$  on  $d_{xy}$  superconductivity.

Although we find a substantial enhancement of pairing in the  $d_{xy}$  channel with  $J'$ , the associated  $T_c$  is yet very low from simple estimates:  $T_c \sim e^{-1/|\lambda_i|} \sim 6 \cdot 10^{-8}t$ , which is tiny even taking the most favorable case of  $J' = 0.3t$  (see Fig. 4) for pairing, for which,  $\lambda_{d_{xy}} \sim -0.06$ .

Small  $T_c$  values have been also found by Motrunich and Lee<sup>17</sup> in the context of  $\text{Na}_x\text{CoO}_2$ , although their couplings are typically larger than ours because, in the case of  $\text{Na}_x\text{CoO}_2$ , several sections of the Fermi surface are connected by the charge ordering wavevector for  $x = 1/3$ . It is worth noting that in our approach we have not considered the renormalization of the quasiparticles, which enhances the effective mass, that occurs close to the charge ordering transition due to  $V$ . This could be taken into account by including self-energy effects in the calculation. One would then have to consider that the hopping amplitudes are effectively renormalized by the quasiparticle weight,  $Z$ , which decreases near the charge instability<sup>7</sup>. This would transform the bare hopping,  $t$ , to  $t_{eff} = Zt$ . Hence, the ratios  $J/t_{eff}$  and  $V/t_{eff}$  would be enhanced, effectively increasing  $|\lambda_{d_{xy}}|$  which would, in turn, significantly increase the estimated  $T_c$ .

#### IV. CONCLUSIONS

In conclusion, we have found that superconductivity with  $d_{xy}$  symmetry induced by charge fluctuations is strengthened by antiferromagnetic spin fluctuations induced by the exchange coupling,  $J'$ , in a  $t - J' - V$  model for quarter-filled systems. This can be intuitively understood by analogy with the more standard case of  $d_{x^2-y^2}$  superconductivity induced by the superexchange coupling  $J$  in the  $t - J$  model if one realizes that the  $J'$  acts in directions rotated by  $45^\circ$  with respect to  $J$ . Both charge and spin fluctuations are then found to work together cooperatively to produce  $d_{xy}$  superconductivity in the quarter-filled  $t - J' - V$  model.

The way superconductivity behaves in the  $t - J' - V$  model proposed here, could be viewed as a two step process in which the charge fluctuations are responsible for the onset of SC in the first place and subsequently the dynamically generated spin exchange coupling  $J'$  would strengthen the binding between electrons forming the Cooper pairs.

Critical temperatures are found to be too small compared to experimental values (which are of the order of a few Kelvin). The smallness of  $T_c$  is related to the small Fermi surface associated with the one-quarter filling of the system. Due to this fact, there are no two points at the Fermi surface connected by the  $(\pi, \pi)$  CO wavevector which makes the interaction less effective in producing Cooper pairs than in nearly antiferromagnetic metals close to half-filling. A similar situation arises in the  $t - J$  model<sup>13</sup> at one-quarter filling in which superconductivity in the  $d_{x^2-y^2}$  channel is found although with rather small attractive effective couplings. Only at dopings close to half-filling (for doping levels of at most 0.15-0.2) the couplings are found to be substantial<sup>18</sup>. This is because, in this case, larger Fermi surface sections are effectively connected by the AF  $(\pi, \pi)$  wavevector.

An important finding that derives from our work is that including  $J'$  is crucial in order to enhance  $T_c$  suf-

ficiently. If only the  $V$  is taken into account, the values of  $T_c$ <sup>7</sup> obtained would be astronomically small as previously noted<sup>7</sup>. A more sophisticated theory including the renormalization of the quasiparticles could enhance the estimates for  $T_c$  even further. Measured effective masses in quarter-filled layered organics correspond to values of about:  $m^*/m = 1 - 2$ , leading to  $J'/t$  larger by a factor of 2. Considering the dependence of  $\lambda_{d_{xy}}$  with  $J'/t$  shown in Fig. 4, this many-body effect can lead to large enhancements in  $T_c$  as  $T_c$  depends exponentially with  $\lambda_{d_{xy}}$ . Hence,  $T_c$ 's of a fraction of a Kelvin can be obtained in the most favorable case, for  $V = 0.5t$  and  $J/t = 0.3t$ , considering  $t \sim 0.1$  eV<sup>2</sup>.

It has been recently suggested by Coldea *et. al.* Ref. [19] that certain experimental observations are consistent with the charge mediated superconductivity scenario. For instance, the unit cell volume of  $\beta''$ -(BEDT-TTF)<sub>4</sub>[(H<sub>3</sub>O)M(C<sub>2</sub>O<sub>4</sub>)<sub>3</sub>]. Y [19] and  $\alpha$ -(BEDT-TTF)<sub>2</sub>MHg(SCN)<sub>4</sub> salts [20], is found to increase from metallic to insulating salts by changing M and Y. Superconducting salts such as  $\alpha$ -(BEDT-TTF)<sub>2</sub>NH<sub>4</sub>Hg(SCN)<sub>4</sub> and the recently analyzed  $\beta''$ -(BEDT-TTF)<sub>4</sub>[(H<sub>3</sub>O)Ga(C<sub>2</sub>O<sub>4</sub>)<sub>3</sub>].C<sub>6</sub>H<sub>5</sub>NO<sub>2</sub> are found to have unit cell volumes right between their respective metallic and insulating salts. Increasing the unit-cell volume is translated to an increase in  $V/t$  as well as in  $J'/t$  within our model which drives the system closer to the charge ordered state. In the critical region between the metal and charge ordered phase,  $V \lesssim V_c$ , superconductivity is predicted to appear<sup>6</sup>.

However, a definitive test for unconventional  $d$ -wave pairing in quasi-two-dimensional quarter-filled organics is yet missing. Possible experimental probes could come

from measurements of the Knight shift and NMR relaxation rate in the metallic phase close to the CO transition. In contrast to the  $\kappa$ -(BEDT-TTF)<sub>2</sub>X superconductors, in which large enhancements of the Korringa ratio are found due to their closeness to a Mott phase, in the quarter-filled systems studied here there should be no enhancement of the Korringa ratio. Finally, the dependence of  $T_c$  on impurities and disorder can also be used to distinguish  $d$ -wave superconductivity from conventional  $s$ -wave pairing as recently pointed out<sup>21</sup>.

### Acknowledgments

J. M. acknowledges financial support from the Ministerio de Ciencia y Tecnología through the Ramón y Cajal program and EU under contract MERG-CT-2004-506177. We acknowledge helpful discussions with L. Manuel, J. Riera, A. Trumper and M. Vojta. R. H. M. acknowledges financial support from the Australian Research Council.

### APPENDIX A: APPENDIX: LARGE- $N$ APPROACH FOR $t - J' - V$ MODEL

In this appendix, we will give a summary of the path integral large- $N$  approach for Hubbard operators<sup>7,11,12</sup> used in the present paper. More detailed version of the formalism including the exchange coupling can be found in<sup>12</sup>.

First we introduce Hubbard operators which are related with the usual fermionic operators by

$$X_i^{0\sigma} = (1 - c_{i\bar{\sigma}}^\dagger c_{i\bar{\sigma}})c_{i\sigma}, \quad X_i^{\sigma 0} = (X_i^{0\sigma})^\dagger, \quad X_i^{\sigma\sigma'} = c_{i\sigma}^\dagger c_{i\sigma'}. \quad (A1)$$

The five Hubbard  $X_i$ -operators  $X_i^{\sigma\sigma'}$  and  $X_i^{00}$  are boson-like and the four Hubbard  $X$ -operators  $X_i^{\sigma 0}$  and  $X_i^{0\sigma}$  are fermion-like. The names fermion-like and boson-like come from the fact that Hubbard operators do not verify the usual fermionic and bosonic commutation relations<sup>22</sup>.

From the above relations we note that  $X_i^{\sigma 0} = \tilde{c}_{i\sigma}^\dagger$  and  $X_i^{\uparrow\downarrow} = S_i^+$ .

The Hubbard operators satisfy:

a)the completeness condition

$$X_i^{00} + \sum_{\sigma} X_i^{\sigma\sigma} = 1, \quad (A2)$$

which is equivalent to imposing that "double occupancy" at each site is forbidden.

b)the commutation rules

$$[X_i^{\alpha\beta}, X_j^{\gamma\delta}]_{\pm} = \delta_{ij}(\delta^{\beta\gamma} X_i^{\alpha\delta} \pm \delta^{\alpha\delta} X_i^{\gamma\beta}) \quad (A3)$$

where the  $+$  sign must be used when both operators are fermion-like, otherwise it corresponds the  $-$  sign.

On the basis of Hubbard  $X$ -operators, the  $t - J' - V$  Hamiltonian (1) is of the form:

$$H(X) = \sum_{\langle ij \rangle, \sigma} (t_{ij} X_i^{\sigma 0} X_j^{0\sigma} + h.c.) + \frac{1}{2} \sum_{\langle ij \rangle, \sigma} J'_{ij} (X_i^{\sigma \bar{\sigma}} X_j^{\bar{\sigma} \sigma} - X_i^{\sigma \sigma} X_j^{\bar{\sigma} \bar{\sigma}}) + \sum_{\langle ij \rangle, \sigma \sigma'} V_{ij} X_i^{\sigma \sigma} X_j^{\sigma' \sigma'} - \mu \sum_{i, \sigma} X_i^{\sigma \sigma} \quad (\text{A4})$$

---

Our starting point is the path integral partition function  $Z$  written in the Euclidean form

---

$$Z = \int \mathcal{D}X_i^{\alpha\beta} \delta[X_i^{00} + \sum_{\sigma} X_i^{\sigma\sigma} - 1] \delta[X_i^{\sigma\sigma'} - \frac{X_i^{\sigma 0} X_i^{0\sigma'}}{X_i^{00}}] \times (\text{sdet} M_{AB})_i^{\frac{1}{2}} \exp \left( - \int d\tau L_E(X, \dot{X}) \right) \quad (\text{A5})$$

The Euclidean Lagrangian  $L_E(X, \dot{X})$  in (A5) is

$$L_E(X, \dot{X}) = \frac{1}{2} \sum_{i, \sigma} \frac{(\dot{X}_i^{0\sigma} X_i^{\sigma 0} + \dot{X}_i^{\sigma 0} X_i^{0\sigma})}{X_i^{00}} + H(X) \quad (\text{A6})$$

In this path integral we associate Grassmann and usual bosonic variables with Fermi-like and boson-like  $X$ -operators, respectively.

It is worth noting at this point that the path integral representation of the partition function (A5), looks different to that usually found in other solid state problems. The measure of the integral contains additional constraints as well as a determinant,  $(\text{sdet} M_{AB})_i^{\frac{1}{2}}$ . Also the kinetic term of the Lagrangian (A6) is non-polynomial. The determinant reads

$$(\text{sdet} M_{AB})_i^{\frac{1}{2}} = 1 / \frac{1}{(-X^{00})^2}, \quad (\text{A7})$$

and is formed by all the constraints of the theory.

We now discuss the main steps needed to introduce a large- $N$  expansion of the partition function (A5). First, we integrate over the boson variables  $X^{\sigma\sigma'}$  using the second  $\delta$ -function in (A5). We extend the spin index  $\sigma = \pm$ , to a new index  $p$  running from 1 to  $N$ . In order to get a finite theory in the  $N \rightarrow \infty$  limit, we re-scale  $t_{ij}$  to  $t_{ij}/N$ ,  $V_{ij}$  to  $V_{ij}/N$  and  $J'_{ij}$  to  $J'_{ij}/N$ . The completeness condition is enforced by exponentiating  $X_i^{00} + \sum_p X_i^{pp} = N/2$ ,

with the help of Lagrangian multipliers  $\lambda_i$ . We write the boson fields in terms of static mean-field values,  $(r_0, \lambda_0)$  and dynamic fluctuations

$$\begin{aligned} X_i^{00} &= N r_0 (1 + \delta R_i) \\ \lambda_i &= \lambda_0 + \delta \lambda_i, \end{aligned} \quad (\text{A8})$$

and, we make the following change of variables

$$\begin{aligned} f_{ip}^+ &= \frac{1}{\sqrt{N r_0}} X_i^{p0} \\ f_{ip} &= \frac{1}{\sqrt{N r_0}} X_i^{0p}, \end{aligned} \quad (\text{A9})$$

where  $f_{ip}^+$  and  $f_{ip}$  are Grassmann variables.

The exchange interactions can be decoupled in terms of the bond variable  $\Delta_{ij}$  through a Hubbard-Stratonovich transformation, where  $\Delta_{ij}$  is the field associated with the quantity  $\sum_p \frac{f_{ip}^+ f_{jp}}{\sqrt{(1+\delta R_i)(1+\delta R_j)}}$ . We write the  $\Delta_{ij}$  fields in term of static mean field values and dynamics fluctuations  $\Delta_i^\eta = \Delta(1 + r_i^\eta + i A_i^\eta)$ , where  $\eta$  can take two values associated with the bond directions  $\eta_1 = (1, 1)$  and  $\eta_2 = (-1, 1)$  in real space.

Introducing the above change of variables into Eq. (A5) and, after expanding the denominators  $1/(1+\delta R)$ , we arrive at the following effective Lagrangian:

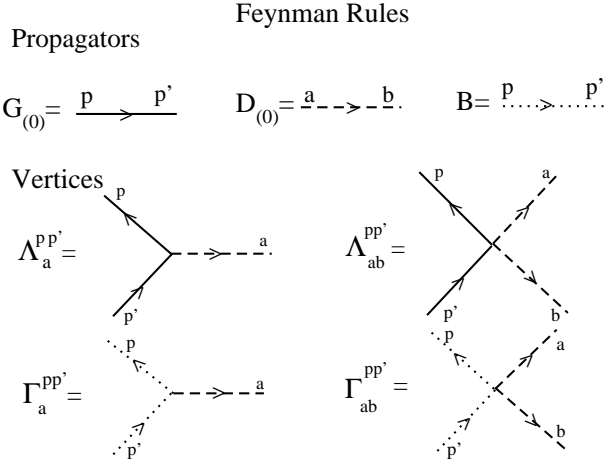


FIG. 5: Summary of the Feynman rules. Solid line represents the propagator  $G_{(0)}$  for the correlated fermion  $X^{0\sigma}$ . Dashed line represents the  $6 \times 6$  boson propagator  $D_{(0)}$  for the 6-component field  $\delta X^a$ . The component (1, 1) of this propagator is directly associated with the  $X^{00}$  charge operator. Dotted line is the propagator  $B$  for the boson ghost field  $\mathcal{Z}_p$ .  $\Lambda_a^{pp'}$  and  $\Lambda_{ab}^{pp'}$  represent the interaction between two fermions  $f_p$  and one and two bosons  $\delta X^a$  respectively.  $\Gamma_a^{pp'}$  and  $\Gamma_{ab}^{pp'}$  represent the interaction between two ghost fields  $\mathcal{Z}_p$  and one and two bosons  $\delta X^a$  respectively.

$$\begin{aligned}
L_{eff} = & -\frac{1}{2} \sum_{i,p} \left( f_{ip}^+ f_{ip} + f_{ip}^+ f_{ip} \right) (1 - \delta R_i + \delta R_i^2) + \sum_{\langle ij \rangle, p} (t_{ij} r_0 f_{ip}^+ f_{jp} + h.c.) - \mu \sum_{i,p} f_{ip}^+ f_{ip} (1 - \delta R_i + \delta R_i^2) \\
& + N r_0 \sum_i \delta \lambda_i \delta R_i + \sum_{i,p} f_{ip}^+ f_{ip} (1 - \delta R_i) \delta \lambda_i + \frac{2N}{J} \Delta^2 \sum_{i\eta} [(r_i^\eta)^2 + (A_i^\eta)^2] \\
& - \Delta \sum_{\langle ij \rangle, p, p'} (f_{ip}^+ f_{jp'} + f_{jp'}^+ f_{ip}) \left[ 1 - \frac{1}{2} (\delta R_i + \delta R_j) + \frac{1}{4} \delta R_i \delta R_j + \frac{3}{8} (\delta R_i^2 + \delta R_j^2) \right] \\
& - \Delta \sum_{\langle ij \rangle, p, p'} (f_{ip}^+ f_{jp'} + f_{jp'}^+ f_{ip}) (r_i^\eta + i A_i^\eta) \left[ 1 - \frac{1}{2} (\delta R_i + \delta R_j) \right] \\
& + N r_0^2 \sum_{\langle ij \rangle} (V_{ij} - \frac{1}{2} J_{ij}) \delta R_i \delta R_j - \sum_{ip} \mathcal{Z}_{ip}^\dagger (1 - \delta R_i + \delta R_i^2) \mathcal{Z}_{ip},
\end{aligned} \tag{A10}$$

where we have changed  $\mu$  to  $\mu - \lambda_0$  and dropped constant and linear terms in the fields.

The last term of (A10) results from the path integral representation of the determinant which uses  $N$ -component boson ghost field  $\mathcal{Z}_p$ <sup>7,11,12</sup>.

Looking at the effective Lagrangian (A10), the Feynman rules can be obtained as usual. The bilinear parts give rise to the propagators and the remaining pieces are represented by vertices. Besides, we assume the equation (A10) written in the momentum space once the Fourier transformation was performed.

To leading order of  $1/N$ , we associate with the  $N$ -

component fermion field  $f_p$ , connecting two generic components  $p$  and  $p'$ , the propagator

$$G_{(0)pp'}(\mathbf{k}, \nu_n) = -\frac{\delta_{pp'}}{i\nu_n - (E_{\mathbf{k}} - \mu)} \tag{A11}$$

which is  $O(1)$  and where  $E_{\mathbf{k}} = -2tr_0(\cos k_x + \cos k_y) - 2\Delta \cos k_x \cos k_y$ , is the electronic dispersion to leading order.

The quantities  $\mathbf{k}$  and  $\nu_n$  are the momentum and the fermionic Matsubara frequency of the fermionic field, respectively.

### a) Irreducible boson self-energy

$$\Pi = \Pi^{(1)} + \Pi^{(2)} + \Pi^{(3)} + \Pi^{(4)}$$

### b) Effective interaction between fermions

$$V_{\text{eff}} =$$

FIG. 6: a) The four different contributions  $\Pi_{ab}^{(i)}$  ( $i = 1, 2, 3, 4$ ) to the irreducible boson self-energy  $\Pi_{ab}$ . b) Effective interaction between fermions. Only two three-legs vertices contribute.

The mean field values  $r_0$  and  $\Delta$  must be determined minimizing the leading order theory. From (A8) and the completeness condition,  $r_0$  is equal to  $\delta/2$ , where  $\delta$  is the hole doping away from half-filling.

On the other hand, minimizing with respect to  $\Delta$  we obtain  $\Delta = \frac{J'}{2} \frac{1}{N_s} \sum_{\mathbf{k}} \cos k_x \cos k_y n_F(E_{\mathbf{k}} - \mu)$ , where  $n_F$  is the Fermi function and  $N_s$  is the number of sites in the Brillouin zone (BZ).

For a given doping,  $\delta$ , the chemical potential  $\mu$  and  $\Delta$  must be determined self-consistently from  $(1 - \delta) = \frac{2}{N_s} \sum_{\mathbf{k}} n_F(E_{\mathbf{k}} - \mu)$

We associate with the six component  $\delta X^a = (\delta R, \delta \lambda, r^1, r^2, A^1, A^2)$  the inverse of the propagator (which is  $O(1/N)$ ), connecting two generic components  $a$  and  $b$ ,

$$D_{(0)ab}^{-1}(\mathbf{q}, \omega_n) = N \begin{pmatrix} \gamma_q & r_0 & 0 & 0 & 0 & 0 \\ r_0 & 0 & 0 & 0 & 0 & 0 \\ 0 & 0 & \frac{4}{J} \Delta^2 & 0 & 0 & 0 \\ 0 & 0 & 0 & \frac{4}{J} \Delta^2 & 0 & 0 \\ 0 & 0 & 0 & 0 & \frac{4}{J} \Delta^2 & 0 \\ 0 & 0 & 0 & 0 & 0 & \frac{4}{J} \Delta^2 \end{pmatrix} \quad (\text{A12})$$

where  $\gamma_{\mathbf{q}} = r_0^2 [4V(\cos(q_x) + \cos(q_y)) - 4J' \cos(q_x) \cos(q_y)]$

The quantities  $\mathbf{q}$  and  $\omega_n$  are the momentum and the Bose Matsubara frequency of the boson field, respectively.

We associate with the  $N$ -component ghost field,  $\mathcal{Z}_p$ , the propagator connecting two generic components  $p$  and  $p'$ ,

$$B_{pp'} = -\delta_{pp'}, \quad (\text{A13})$$

which is  $O(1)$

The non-quadratic terms in (A10) define three and four leg vertices which are  $O(1)$ . (The full expressions for the vertices associated with the large- $N$  approach are given in Ref.[12]). In Fig. 5 the Feynman rules associated with the large- $N$  approach are summarized.

The charge-charge correlation function is directly associated with the element (1,1) of the boson propagator  $D_{(0)ab}(\mathbf{q}, \omega_n)$  (the inverse of Eq. (A12)). As in Ref.[7], up to  $O(1/N)$ ,  $D_0(\mathbf{q}, \omega_n)$  is renormalized to  $D(\mathbf{q}, \omega_n)$  by an infinite series of diagrams of  $O(1/N)$  (Fig. 6a), and reads:

$$D^{-1}(\mathbf{q}, \omega_n) = D_0^{-1}(\mathbf{q}, \omega_n) - \Pi(\mathbf{q}, \omega_n), \quad (\text{A14})$$

where  $\Pi(\mathbf{q}, \omega_n)$  is the boson self-energy for which explicit expressions are given in Ref. 11.

The superconducting effective interaction between fermions,  $V_{\text{eff}}(\mathbf{q}, \omega_n)$ , can be calculated using the Feynman rules of Fig. 5. Fig. 6b) represents the diagram involved in the calculation of  $V_{\text{eff}}(\mathbf{q}, \omega_n)$ . The analytical expression for this diagram is  $V_{\text{eff}} = \Lambda_a D_{ab} \Lambda_b$  where  $D_{ab}$  is the propagator of the bosonic field which contains the irreducible self energies of Fig. 6a and  $\Lambda_a$  is the three leg vertex of Fig. 5. Looking at the order of the propagators and vertices we see that  $V_{\text{eff}}(\mathbf{q}, \omega_n)$  is  $O(1/N)$ .

To conclude this appendix we make contact with closely related approaches such as slave boson formulations. In contrast to slave boson theories: (a) Greens functions are calculated in terms of the original Hubbard operators, (b) fermions,  $f_{ip}$ , appearing in the theory are proportional to the Fermi-like  $X$ -operator  $X^{op}$  (see (A9)) to all orders in the  $1/N$  expansion; not only to leading order<sup>13</sup>, (c) as our path integral is written in terms of  $X$ -operators we do not need to introduce *a priori* any decoupling scheme, and (d)  $r_0$  is the mean value of  $X^{00}$  which is a real field associated with the number of holes (see Eq. (A8)) and not with the number of holons. At leading order ( $N \rightarrow \infty$  or  $O(1)$ ) and  $V = 0$ , our formalism is equivalent to slave boson approaches. However, at the next to leading order ( $O(1/N)$ ), (which is necessary to calculate one-electron properties such as the electron self energy  $\Sigma(\mathbf{k}, \omega)$  and the electron spectral function  $A(\mathbf{k}, \omega)$ ), the two formulations do not coincide. The



differences between the two formulations are not yet completely established. Our theory has the *advantage* that it does not require the introduction of gauge fields like in slave boson approaches. Hence, through order  $O(1/N)$  we do not need to take care of gauge fluctuations nor Bose condensation (note that Eq. (A8) does not mean

Bose condensation). This is important because for the doped Hubbard model the gauge fluctuations are known to significantly change the physics. Careful numerical work will determine the improvements of the present approach with respect to slave boson formulations.

- 
- <sup>1</sup> T. Ishiguro, K. Yamaji, and G. Saito, *Organic Superconductors*, 2nd ed. (Springer-Verlag) Berlin (1998).  
<sup>2</sup> R. H. McKenzie *et. al.*, Phys. Rev. B **64**, 085109 (2001).  
<sup>3</sup> H. Kino and H. Fukuyama, J. Phys. Soc. Jpn. **65** 2158 (1996).  
<sup>4</sup> H. Seo, J. Phys. Soc. Jpn. **69**, 805 (2000).  
<sup>5</sup> M. Calandra, J. Merino and R. H. McKenzie, Phys. Rev. B **66**, 195102 (2002).  
<sup>6</sup> J. Merino and R. H. McKenzie, Phys. Rev. Lett. **87**, 237002 (2001).  
<sup>7</sup> J. Merino, A. Greco, R. H. McKenzie, and M. Calandra, Phys. Rev. B **68**, 245121 (2003). Note that the captions of Fig. 15 and Fig. 16 in this reference are interchanged.  
<sup>8</sup> M. Dressel *et. al.*, Phys. Rev. Lett. **90**, 167002 (2003).  
<sup>9</sup> A. Kobayashi, *et. al.*, J. Phys. Soc. Jpn. **73**, 1115 (2004).  
<sup>10</sup> Y. Ohta, *et. al.*, Phys. Rev. B **50** 13594 (1994).  
<sup>11</sup> A. Foussats and A. Greco, Phys. Rev. B **65**, 195107 (2002).  
<sup>12</sup> A. Foussats and A. Greco, Phys. Rev. B (2004), *in press*.  
<sup>13</sup> M. Grilli and G. Kotliar, Phys. Rev. Lett. **64**, 1170(1990).  
<sup>14</sup> G. Kotliar and J. Liu, Phys. Rev. Lett. **61**, 1784 (1988).  
<sup>15</sup> M. Vojta, Phys. Rev. B **66** 104505 (2002).  
<sup>16</sup> T. Hanaguri, *et. al.*, Nature **430** 1001 (2004).  
<sup>17</sup> O. Motrunich and P. A. Lee, Phys. Rev. B. **70**, 024514 (2004).  
<sup>18</sup> A. Greco and R. Zeyher, Eur. Phys. J. B **6**, 473 (1998).  
<sup>19</sup> A. I. Coldea, *et. al.* submitted to Phys.Rev. B.  
<sup>20</sup> N. Drichko, *private communication*.  
<sup>21</sup> B. J. Powell and Ross H. McKenzie, Phys. Rev. B **69** 024519 (2004).  
<sup>22</sup> J. Hubbard, Proc. R. Soc. London, Ser. A **276**, 238(1963).